Critical endpoint of 4-flavor QCD on the lattice

Hiroshi Ohno[1,2]

in collaboration with

Y. Kuramashi[1,3], Y. Nakamura[3] and S. Takeda[4]

[1]CCS, University of Tsukuba, [2]Brookhaven National Laboratory,

[3]RIKEN AICS, [4]Kanazawa University

CPOD 2017

Stony Brook University, NY, USA

August 9, 2017

Plan of this talk

- Introduction
  - Order of phase transitions of QCD at $\mu = 0$
  - An issue in 3-flavor QCD on the lattice
  - Motivation for 4-flavor QCD
- Methods
  - Finite size scaling analysis & the kurtosis intersection method
- Numerical results
- Summary & outlook

Expected order of phase transitions of QCD at μ = 0

R. D. Pisarski and F. Wilczek, PRD 29 (1984) 338

- Quenched QCD (top-right corner)
  - **1st order**
- 2-flavor at $m = 0$ (top-left corner)
  - **1st order** if $U(1)_A$ is effectively restored
  - **2nd order** if $U(1)_A$ is broken
  - Different lattice results

S. Sharma's talk
Wed. @16:00

- 3-flavor at $m = 0$ (bottom-left corner)
  - **1st order**
- Physical point
  - **crossover**
  - many lattice results suggested

Columbia plot

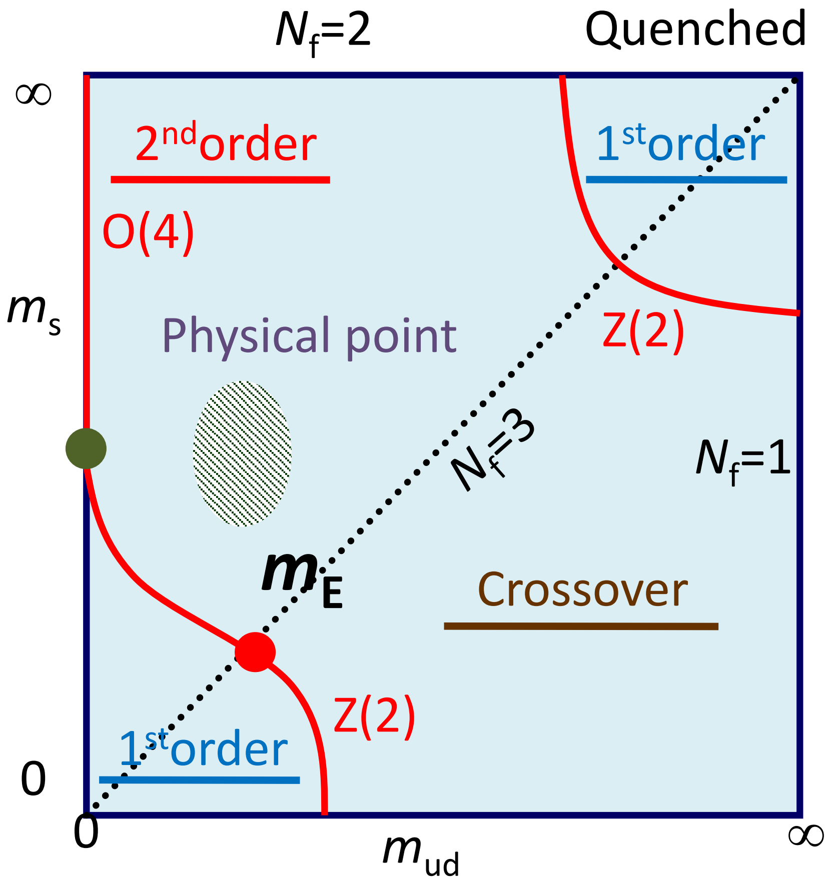

Critical endpoint in 3-flavor QCD

- Phase transition of 3-flavor QCD
  - expected to be **1st order** at $m = 0$
  - **2nd order** critical endpoint at $m = m_E$
  - **crossover** $m > m_E$

- **The location of m_E is still not conclusive!**

Columbia plot

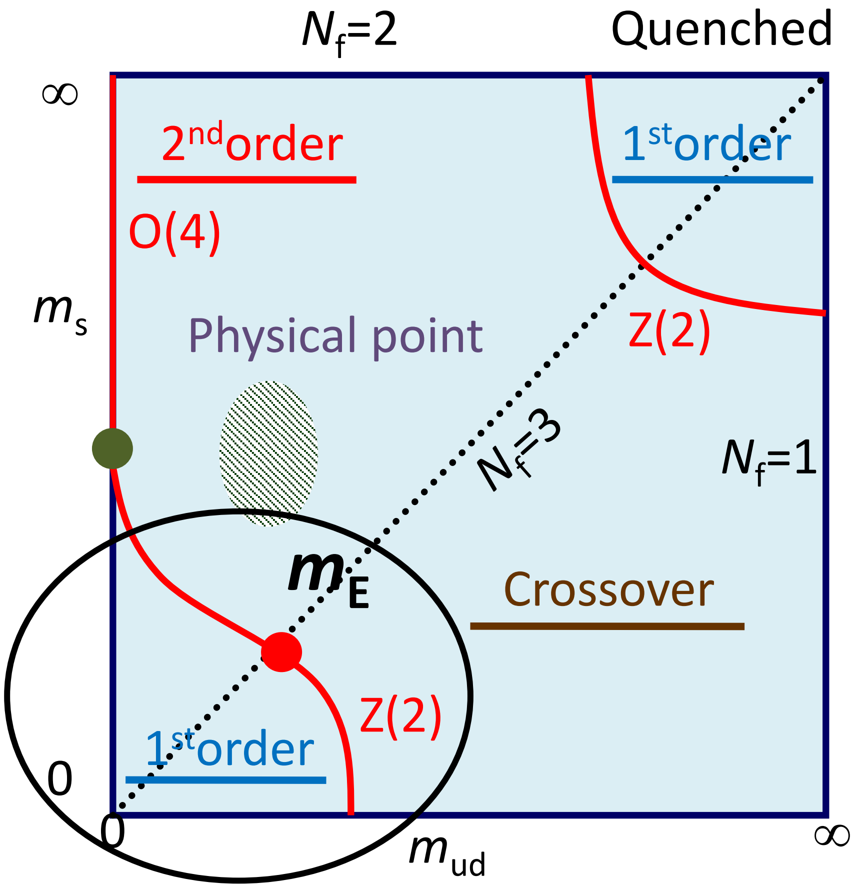

Lattice studies so far

Action	N_t	m^E_π	Ref.
Staggered, standard	4	290 MeV	Karsch et al '01, Liao '01
Staggered, p4	4	67 MeV	Karsch et al '04
Staggered, standard	6	150 MeV	de Forcrand et al '07
Staggered, HISQ	6	< 50 MeV	Ding et al '17
Staggered, stout	4-6	~ 0	Varnhorst '14
Wilson, standard	4	< 670 MeV	Iwasaki et al, '96
Wilson, clover	6-8	300 MeV	Nakamura et al, '14
Wilson, clover	4-10	< 170 MeV	Jin et al, '17

m_E gets smaller for finer lattices and more improved actions
There is clear difference between staggered and Wilson results

A staggered result in 4-flavor QCD

- 4-flavor QCD
  - 1^{st} order phase transition is expected at $m = 0$
  - Stronger phase transition compared to $N_f = 3$
    → larger m_E
    → less expensive computation
  - No rooting issue
  - A good analogue to understand 3-flavor results

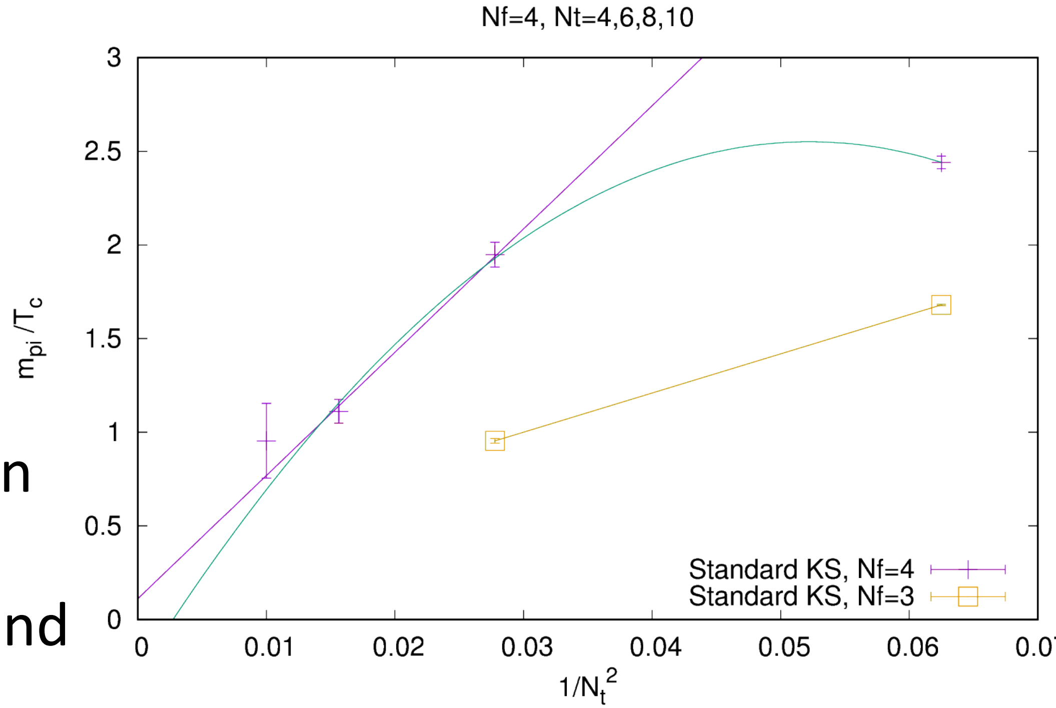

P. de Forcrand and M. D'Elia, PoS LATTICE2016 (2017) 081

- **Similar behavior as $N_f = 3$**
  - **quite small m^E_π in the continuum limit**
    → important to crosscheck also with Wilson-type quarks

Our simulation setup (1)

- Iwasaki gauge + $O(a)$-improved Wilson quarks with 4 degenerate flavors
  - **C_{sw} has been non-perturbatively determined in $N_f = 4$**
- Three different cutoffs towards the continuum limit
  - $N_t = 4$, 6 and 8
  - $N_t = 8$ results are still very preliminary
- Three different β values at each N_t
  - β = 1.61, 1.62 and 1.64 at $N_t = 4$
  - β = 1.67, 1.68 and 1.69 at $N_t = 6$
  - β = 1.66, 1.675 and 1.68 at $N_t = 8$
- Five different κ values at each β
- Zero temperature simulations also have been done on a $16^3 \times 32$ lattice for scale setting (t_0 and m_{PS})

Our simulation setup (2)

- Chiral condensate and its cumulants
  - Up to 4th order, i.e. susceptibility, skewness and kurtosis
  - Traces, e.g. TrD^{-n} for n = 1, 2, 3 and 4, measured with 10 noises
- Multi-ensemble reweighting for κ
  - to improve signal
- The kurtosis intersection method to find critical endpoints

Finite size scaling analysis (1)

For a scaling factor $b = L$, the free energy scales as

t : reduced temperature

h : external magnetic field

L : lattice size

$$F(t, h, L^{-1}) = F(tL^{y_t}, hL^{y_h}, 1)$$

For simplicity thinking about a purely magnetic observable $\mathcal{M}$

Susceptibility scales as

$$\chi_{\mathcal{M}}(t, 0, L^{-1}) = L^{-d} \frac{\partial^2}{\partial h^2} F(t, 0, L^{-1})$$
$$= L^{-d+2y_h} \frac{\partial^2}{\partial h^2} F(tL^{y_t}, 0, 1)$$

$$\chi_{\mathcal{M}}(0, 0, L^{-1}) \propto L^{\gamma/\nu}$$

$$\gamma/\nu = -d + 2y_h$$

Finite size scaling analysis (2)

Similarly, kurtosis scales as

$$K_{\mathrm{M}}(t,0,L^{-1}) = \frac{\frac{\partial^4}{\partial h^4}F(t,0,L^{-1})}{\left[\frac{\partial^2}{\partial h^2}F(t,0,L^{-1})\right]^2} = \frac{\frac{\partial^4}{\partial h^4}F(tL^{y_t},0,1)}{\left[\frac{\partial^2}{\partial h^2}F(tL^{y_t},0,1)\right]^2}$$

For small tL^{y_t}

$$\Rightarrow \quad K_{\mathrm{M}}(t,0,L^{-1}) = \frac{\frac{\partial^4}{\partial h^4}F(0,0,1)}{\left[\frac{\partial^2}{\partial h^2}F(0,0,1)\right]^2} + c_K tL^{1/\nu} + O((tL^{1/\nu})^2)$$

$1/\nu = y_t$

This means that there is no volume dependence at *t* = 0

For general observable there is still volume dependence even at t =0.
However this can be irrelevant for sufficiently large volume

Kurtosis intersection method

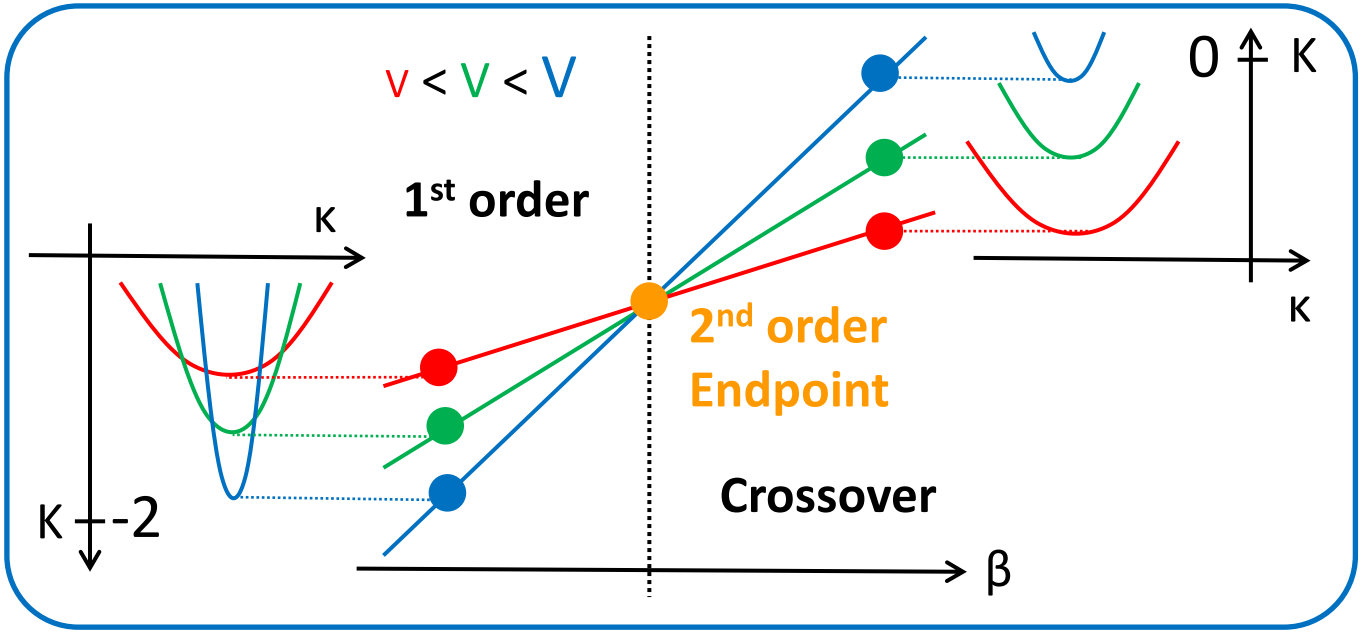

Location of the critical endpoint can be found by looking for a point where kurtosis has no volume dependence.
→ Searching for an intersection point of lines of kurtosis minima in various volumes

An example of cumulants at $N_t = 4$

$\beta = 1.62$

$N_s = 8$

$N_s = 10$

$N_s = 12$

dotted curves: reweighting

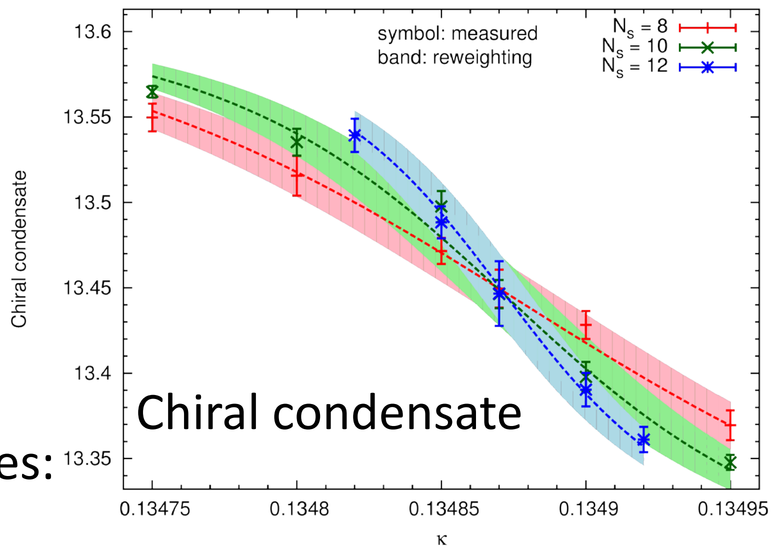

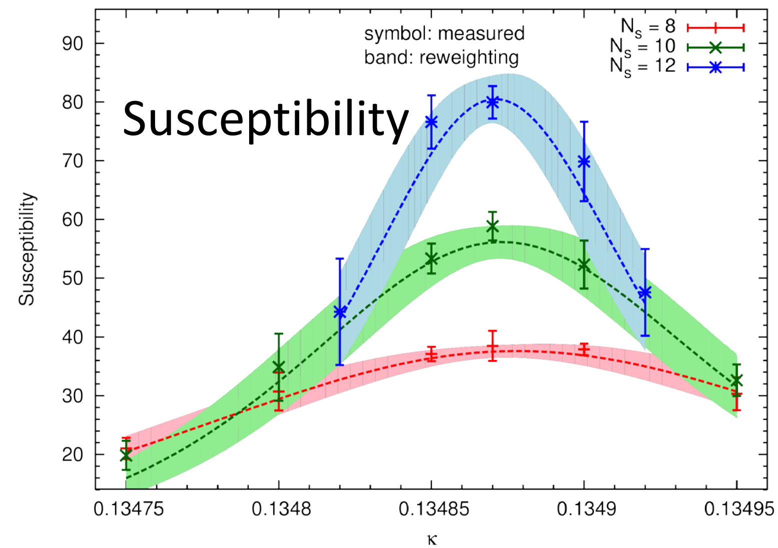

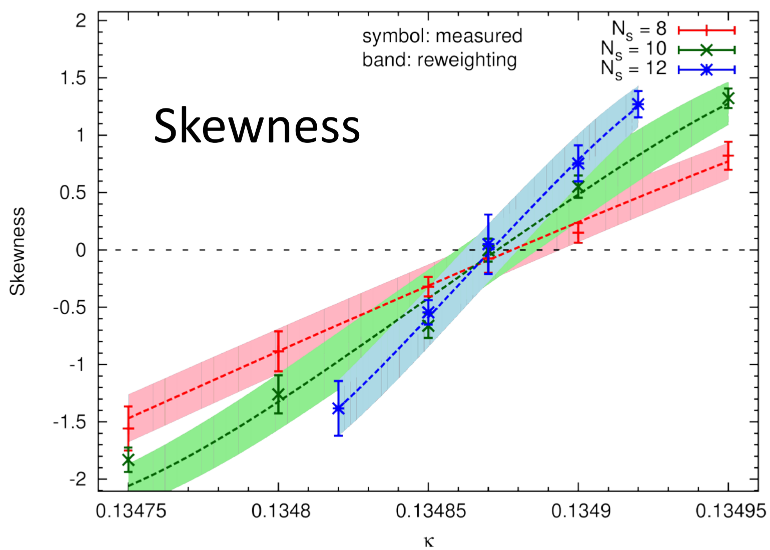

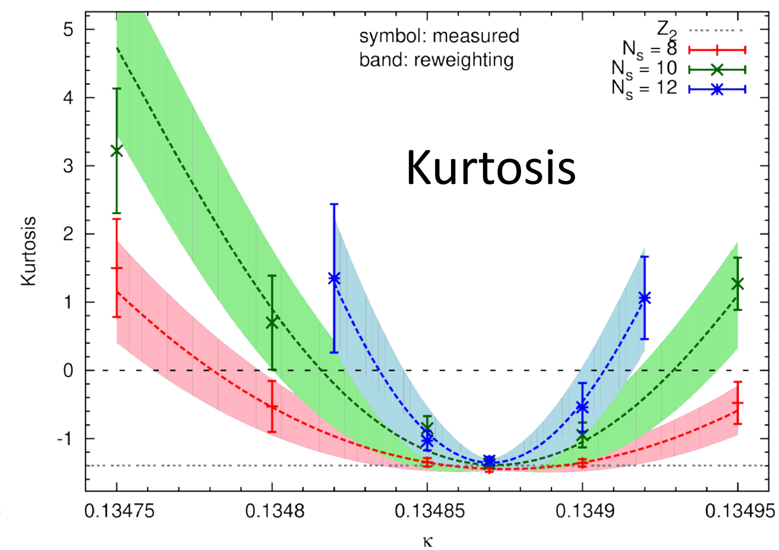

An example of cumulants at $N_t = 6$

$\beta = 1.68$

$N_s = 10$

$N_s = 12$

$N_s = 16$

dotted curves: reweighting

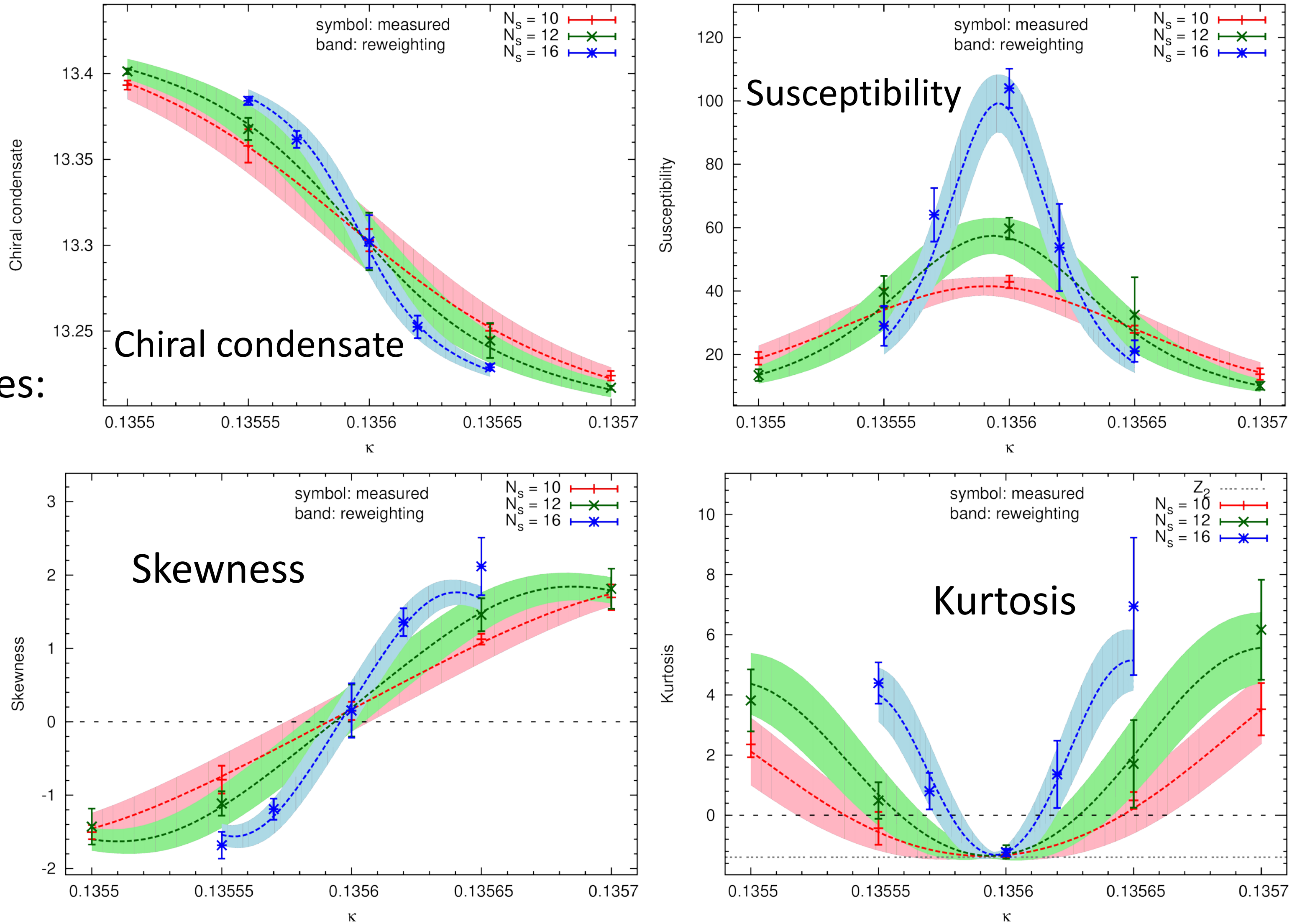

An example of cumulants at $N_t = 8$

$\beta = 1.675$

$N_s = 16$

$N_s = 20$

$N_s = 24$

dotted curves: reweighting

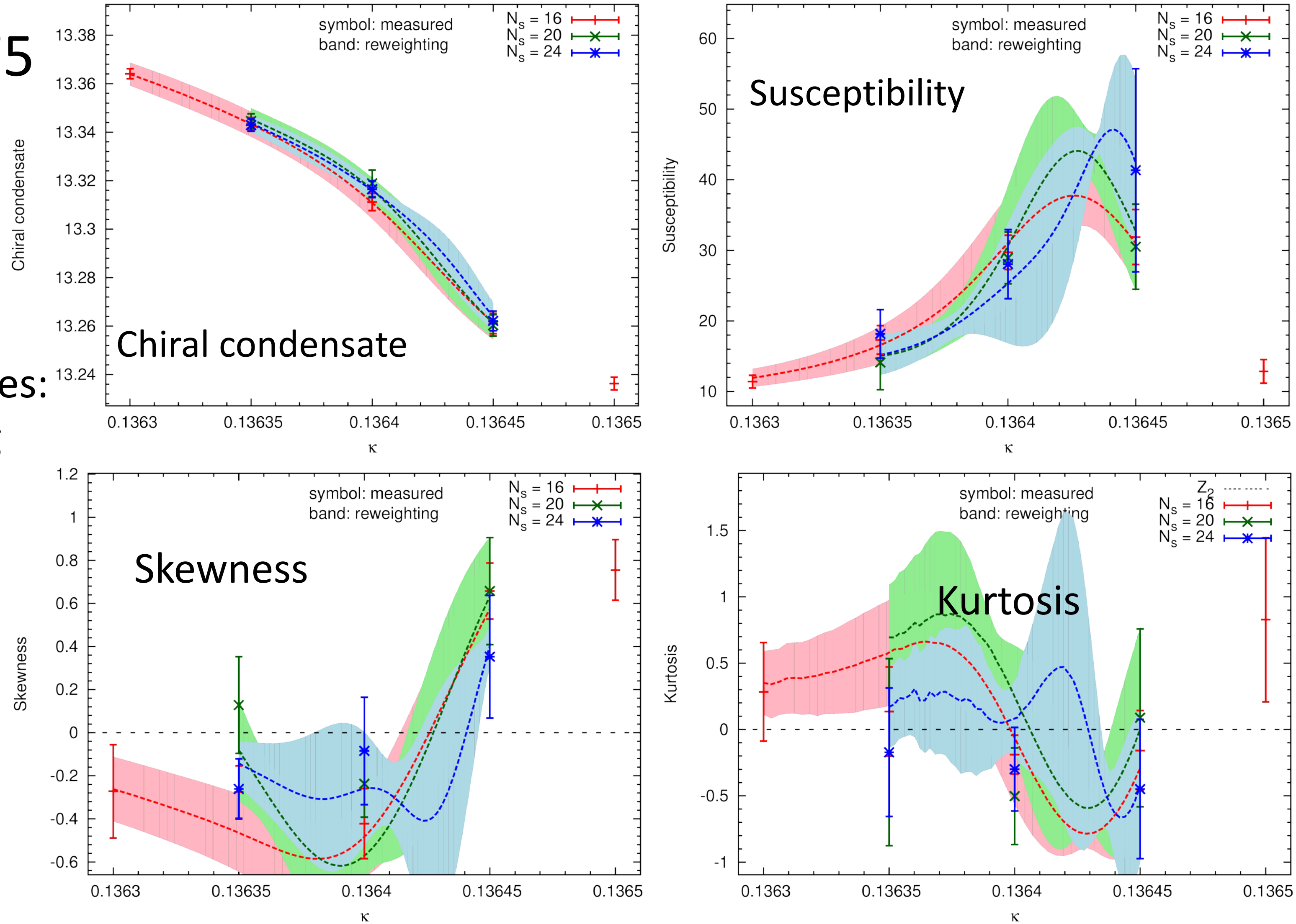

Results of kurtosis intersections

Fit ansatz: $K_t(\beta) = K_E + aN_s^{1/\nu}(\beta - \beta_E)$

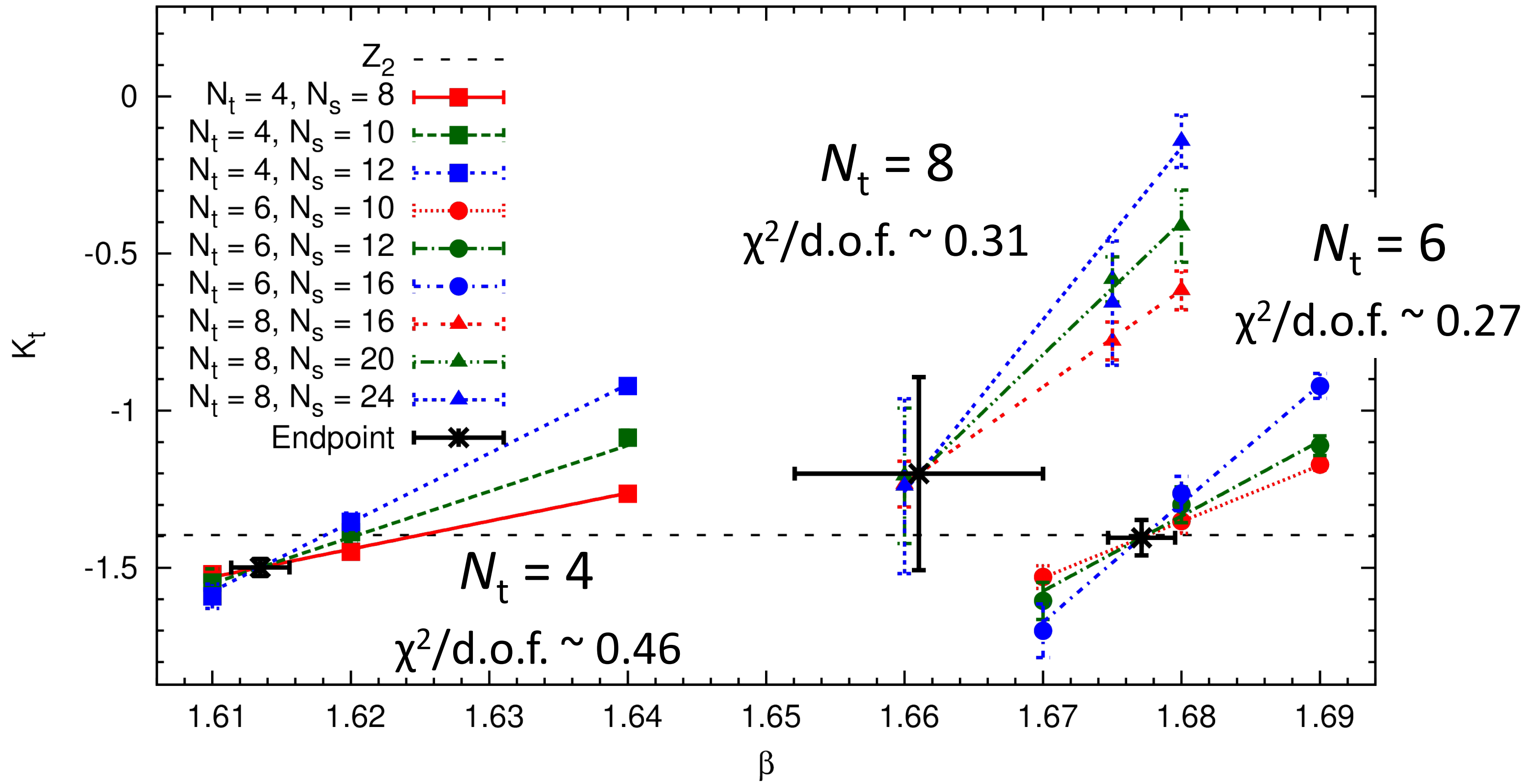

***K_E* slightly deviates from that of Z_2 at *N_t* = 4 and 8 while it is consistent with Z_2 at *N_t* = 6.**
ν = 0.45(4), 0.63(13) and 0.71(33) at *N_t* = 4, 6 and 8, respectively. Cf) ν = 0.630 for Z_2

Further universality check with susceptibilities

Fit ansatz: $\chi_t(N_s) = aN_s^b$

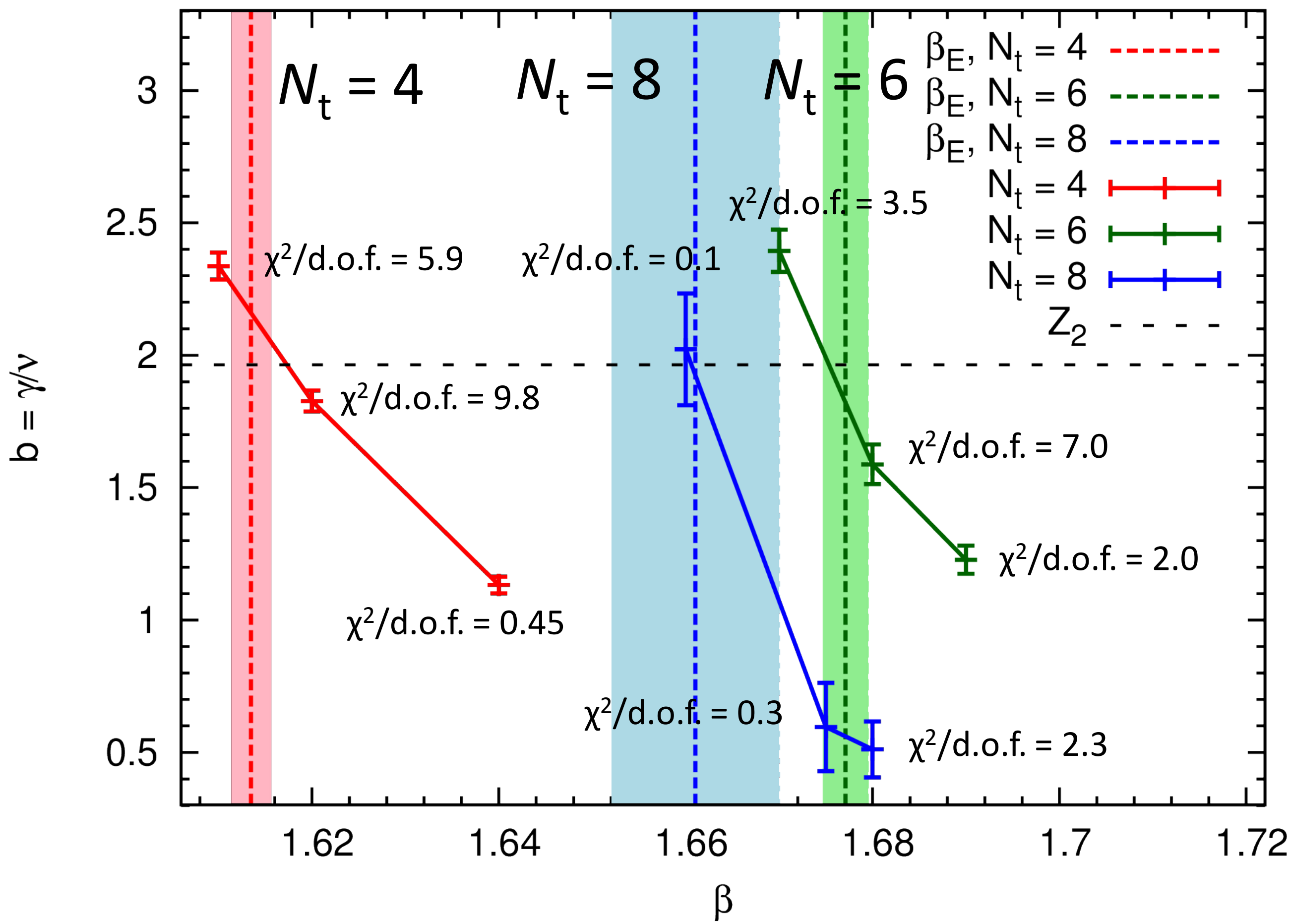

***b* at the endpoint is larger than that of Z_2 at N_t = 4 while it is consistent with Z_2 at N_t = 6 and 8.**

Critical endpoints in N_f = 4 QCD

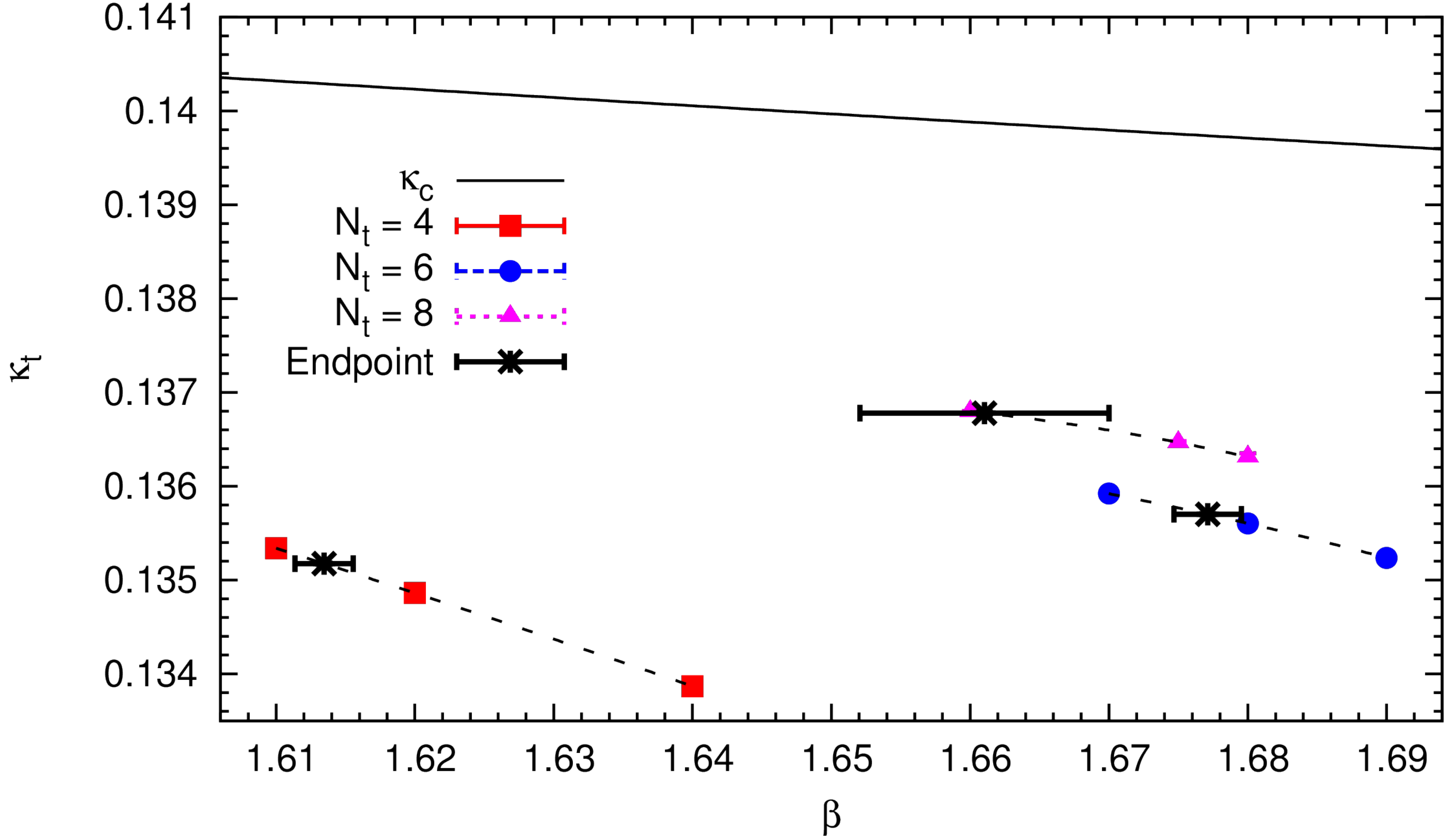

Cutoff dependence of critical endpoints

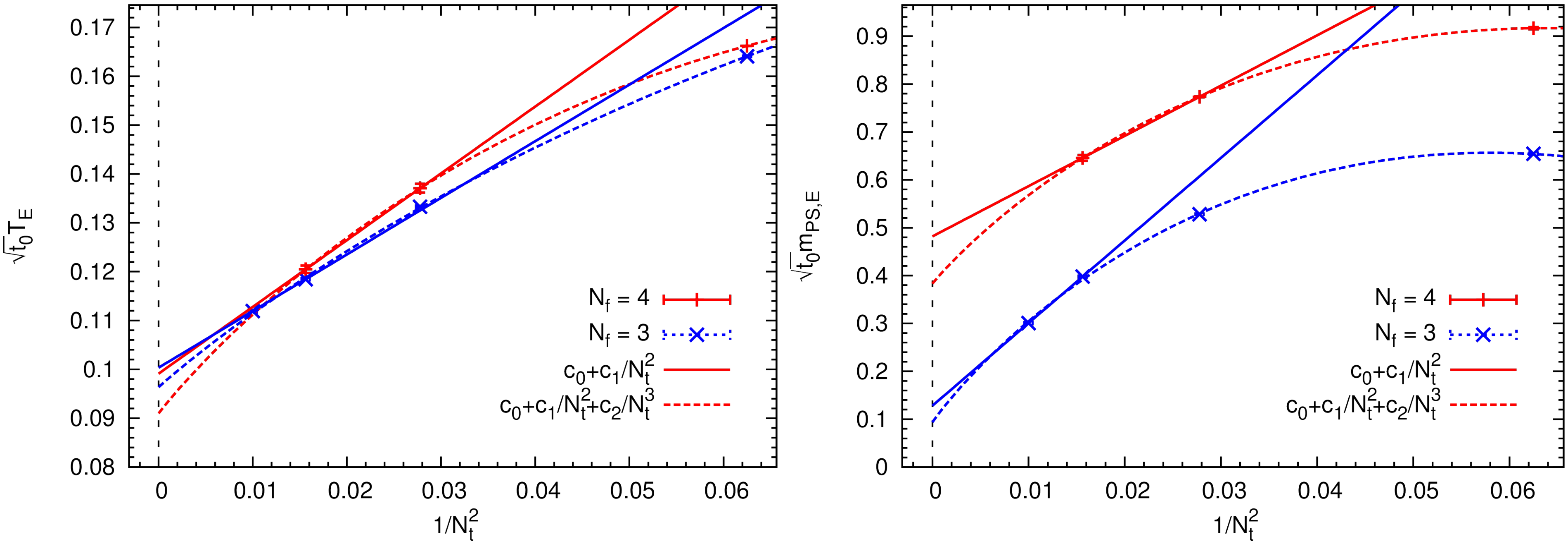

N_f = 3 results: X.-Y. Jin *et al.*, arXiv:1706.01178 [hep-lat]

N_f = 4 results have similar cutoff dependence as those of N_f = 3.
$m_{PS,E}$ in N_f = 4 is larger than that in N_f = 3 as expected.
Further studies at larger N_t (on finer lattices) are needed for the reliable continuum limit.

Comparison with staggered quark results

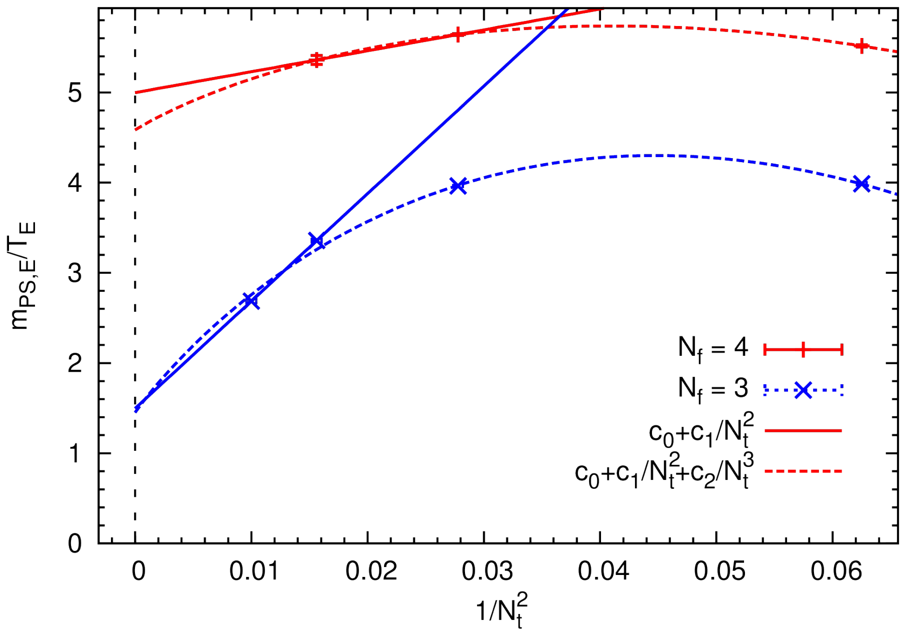

Staggerd results:
P. de Forcrand and M. D'Elia,
PoS LATTICE2016 (2017) 081

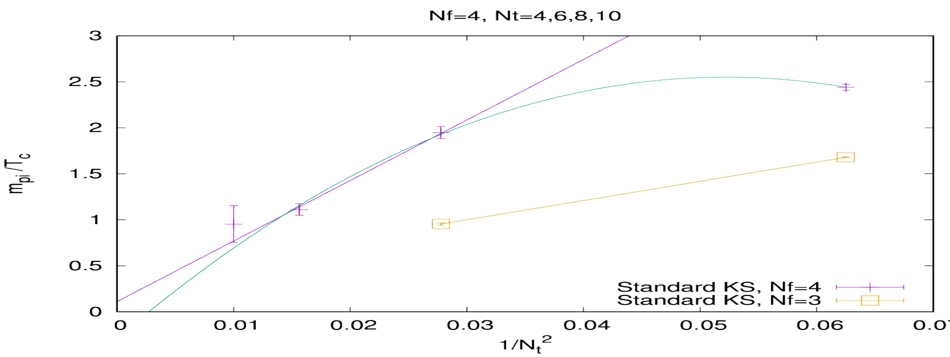

Similarly to the N_f = 3 case, there are different scaling behaviors to the continuum limit between the Wilson and staggered quarks in N_f = 4.

Summary

- Critical endpoints in N_f = 4 QCD has been studied.
- Larger $m_{PS,E}$ has been observed in N_f = 4 than in N_f = 3.
- We found a similar scaling behavior to $a \to 0$ as shown in N_f = 3.
- The scaling behavior is also different from that of the staggered quarks.

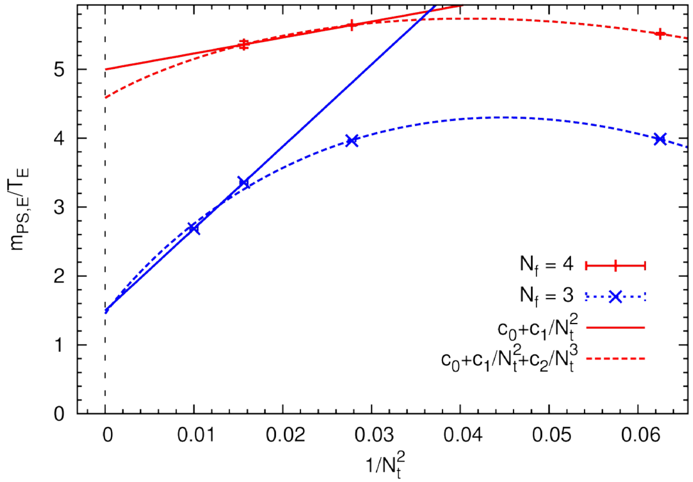

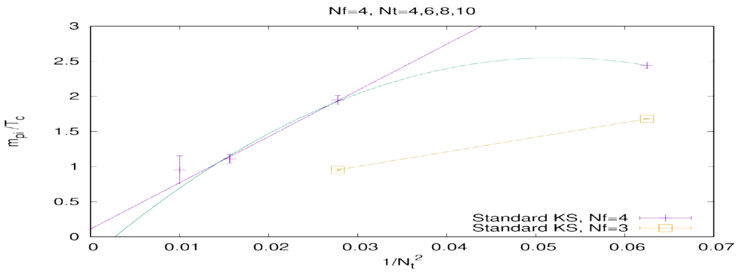

Future plan

- Further studies are needed for the reliable continuum limit.
- More statistics at $N_t = 8$
- Simulations on finer lattices

End

Backup slides

Cumulants at $N_t = 4$, $\beta = 1.61$

$N_s = 8$

$N_s = 10$

$N_s = 12$

dotted curves: reweighting

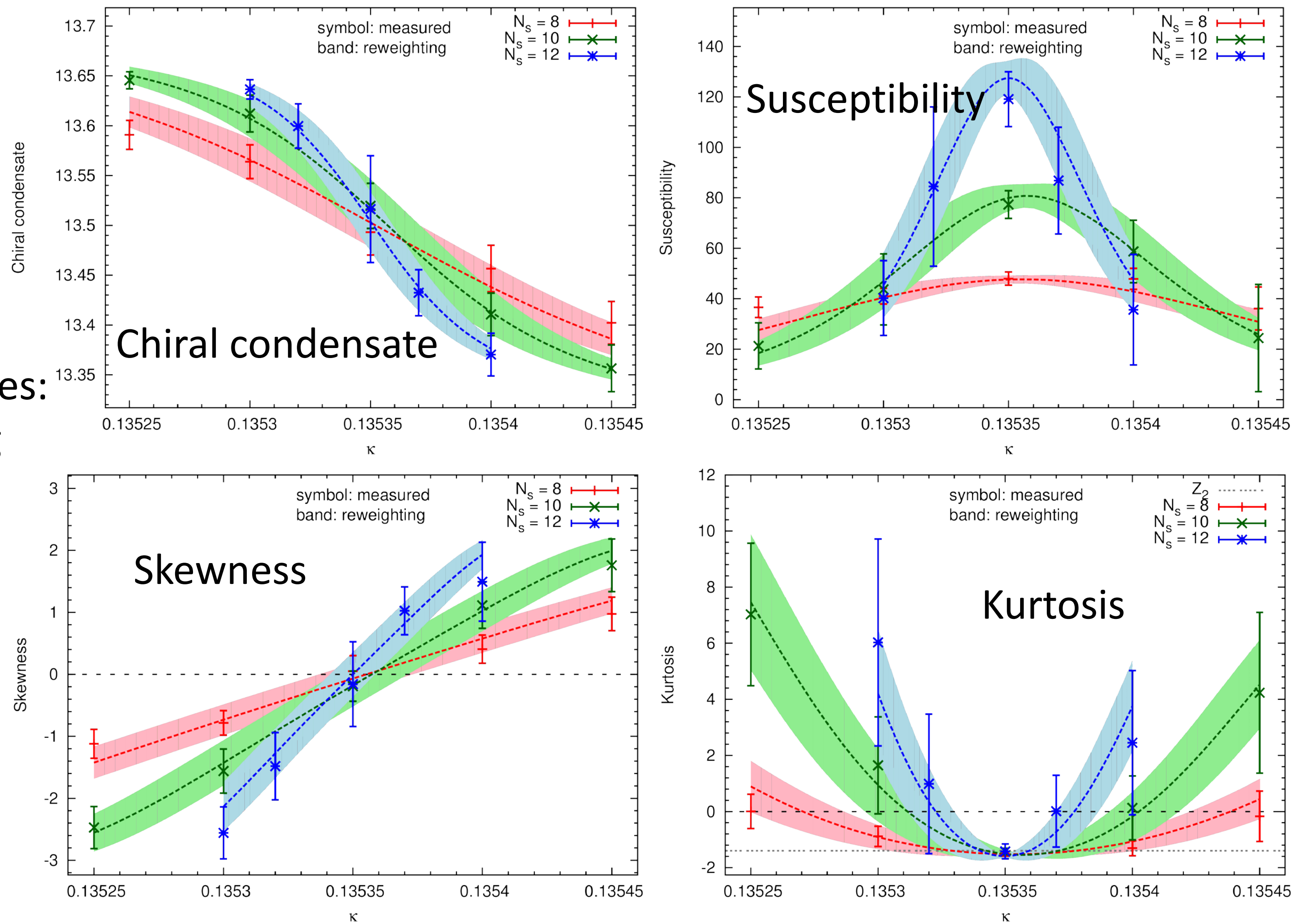

Cumulants at $N_t = 4$, $\beta = 1.64$

$N_s = 8$
$N_s = 10$
$N_s = 12$

dotted curves: reweighting

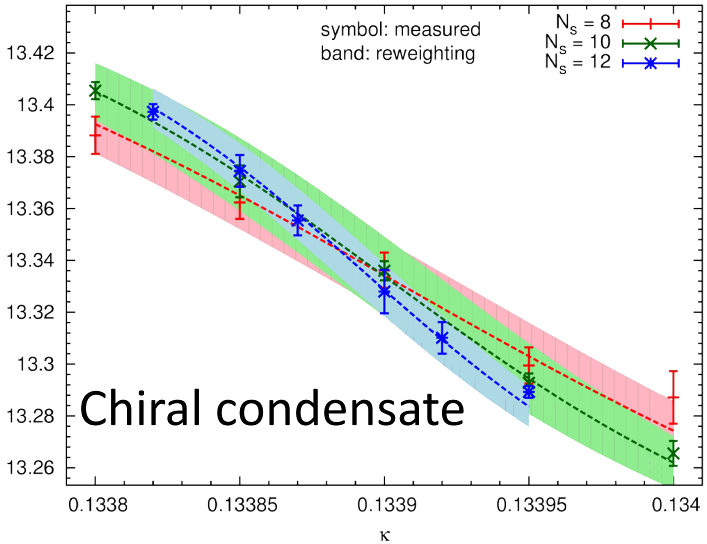

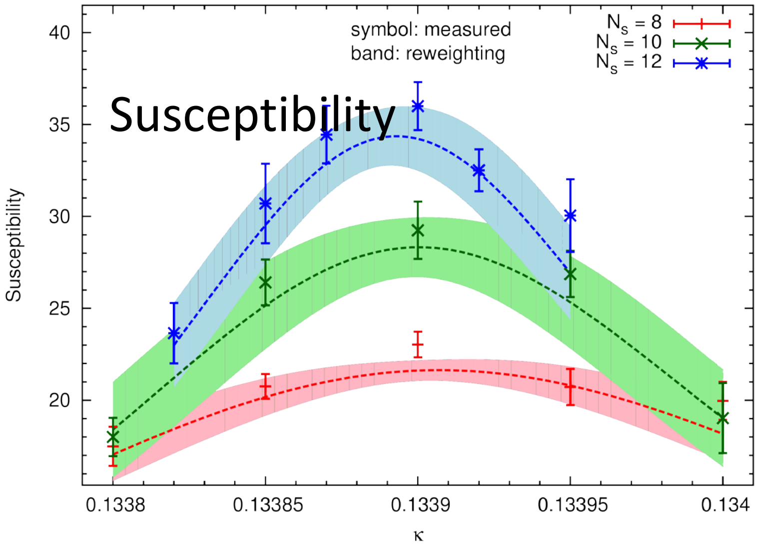

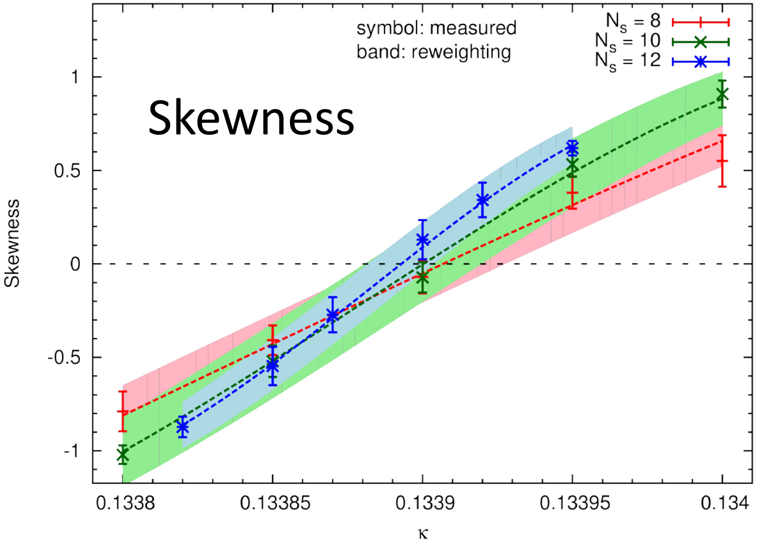

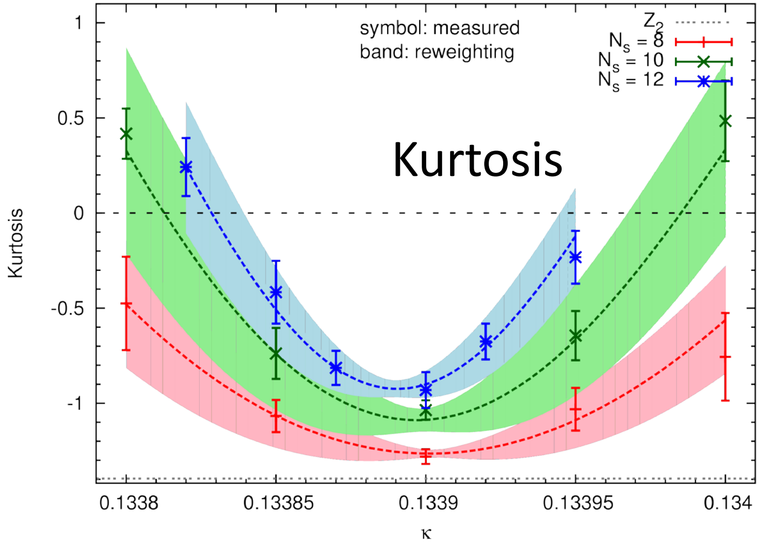

Cumulants at $N_t = 6$, $\beta = 1.67$

$N_s = 10$

$N_s = 12$

$N_s = 16$

dotted curves:
reweighting

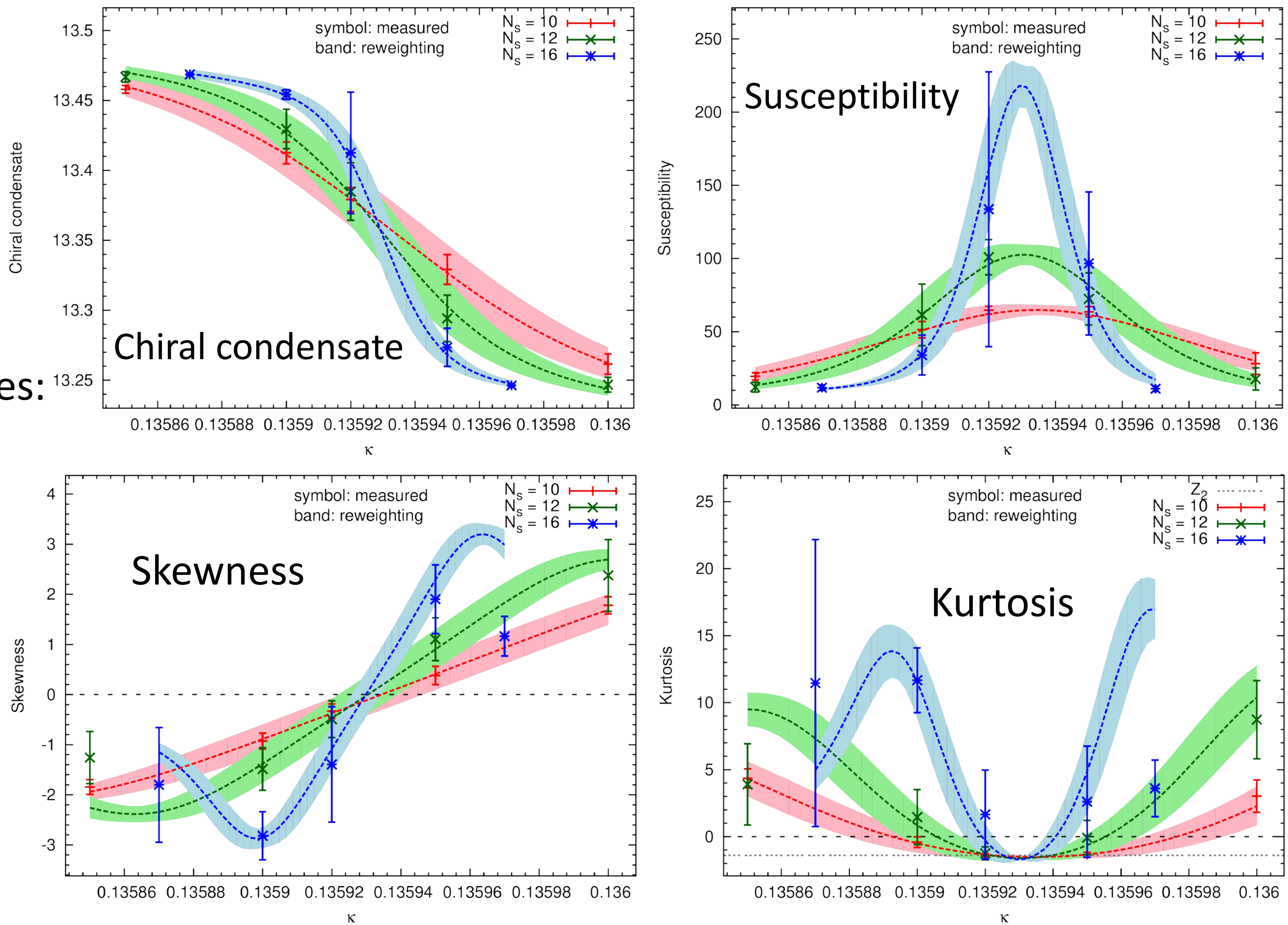

Cumulants at $N_t = 6$, $\beta = 1.69$

$N_s = 10$
$N_s = 12$
$N_s = 16$

dotted curves: reweighting

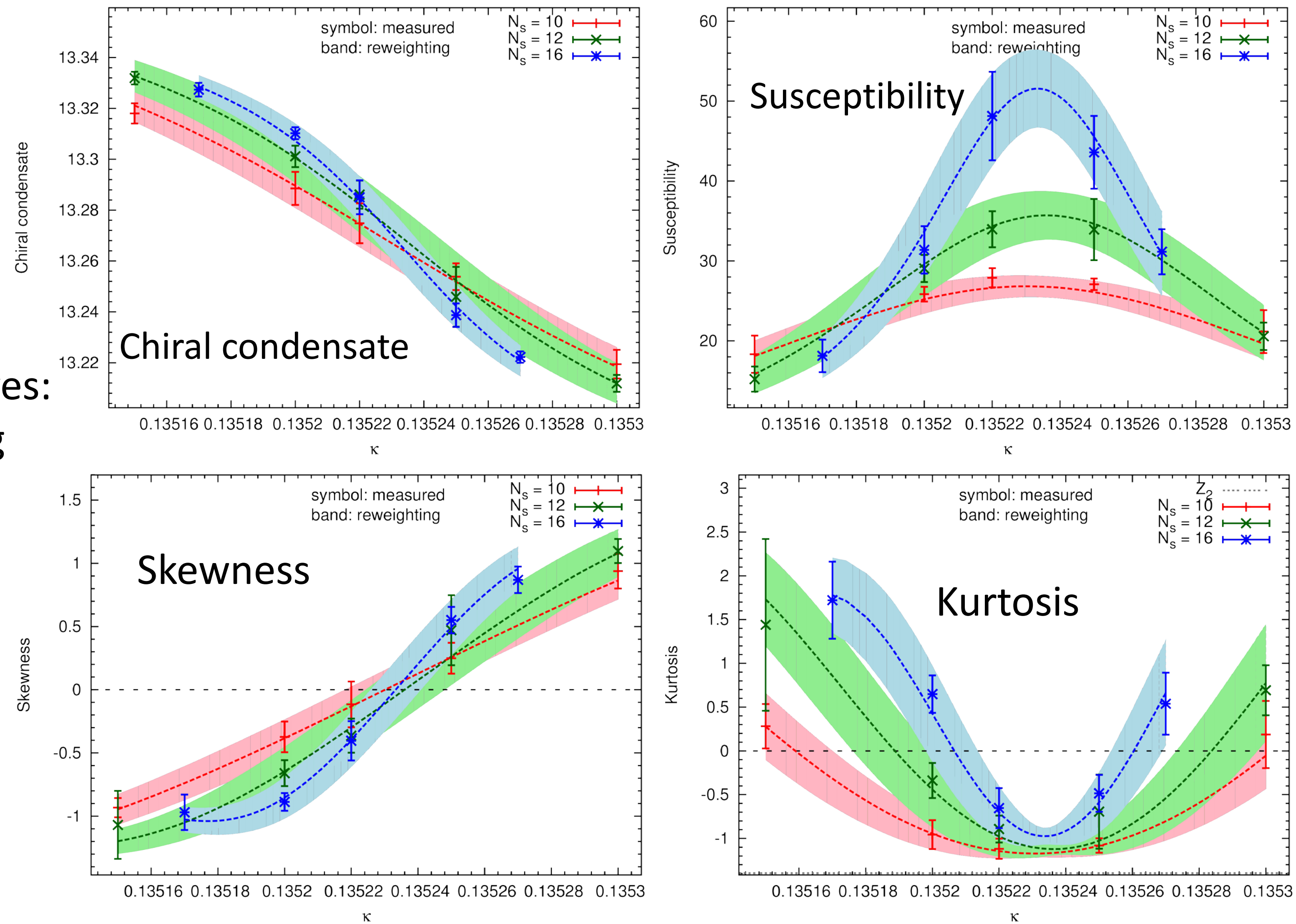

Cumulants at $N_t = 8$, $\beta = 1.66$

$N_s = 16$

$N_s = 20$

$N_s = 24$

dotted curves: reweighting

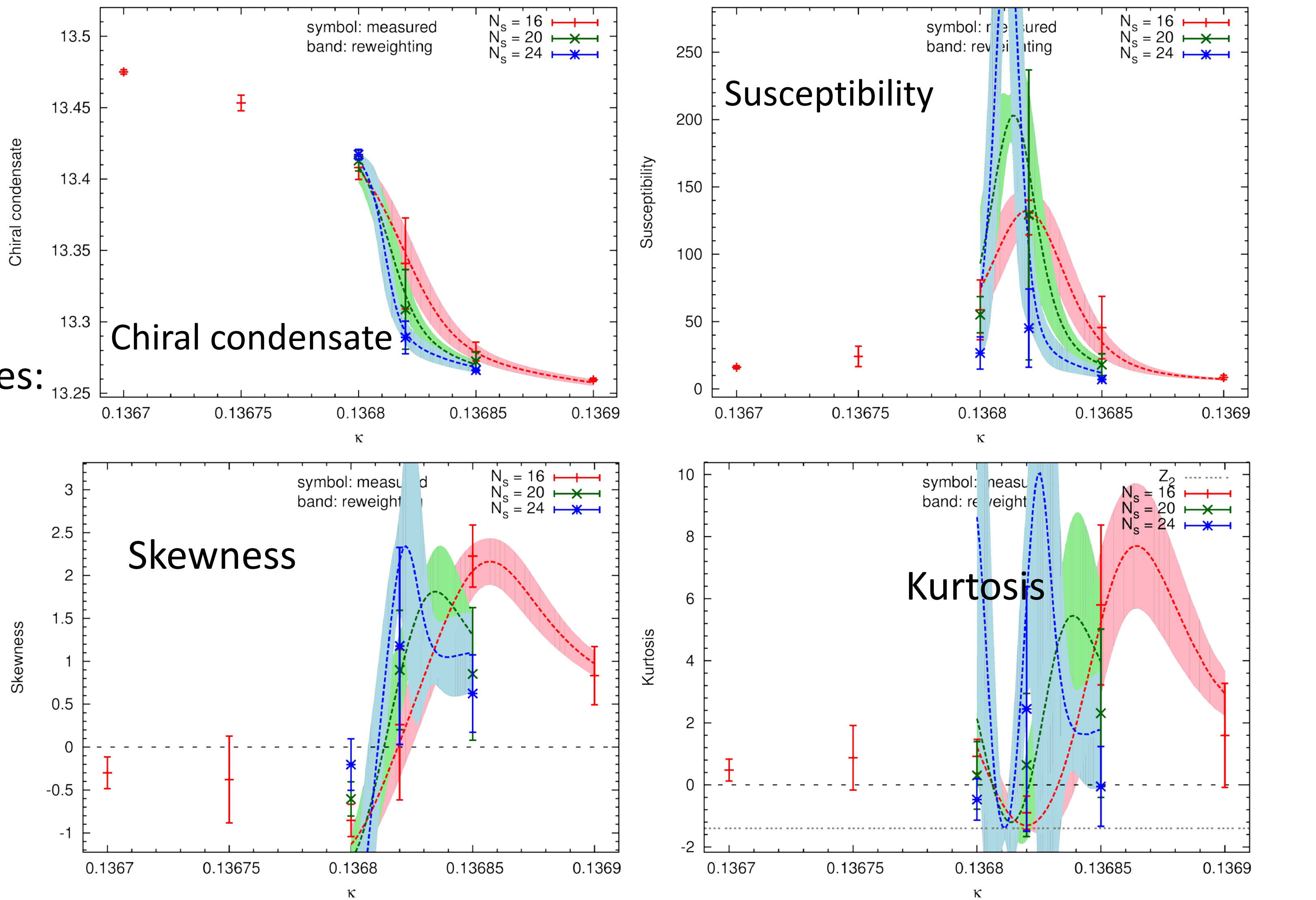

Cumulants at $N_t = 8$, $\beta = 1.68$

$N_s = 16$

$N_s = 20$

$N_s = 24$

dotted curves: reweighting